Hyperfine Interact (2016) 237: 3
DOI 10.1007/s10751-016-1264-y

Magnetic nanoparticles coated with polyaniline to stabilize immobilized trypsin

J. C. Maciel[1] · A. A. D. Mercês[2] · M. Cabrera[2] · W. T. Shigeyosi[3] · S. D. de Souza[4] · M. Olzon-Dionysio[4] · J. D. Fabris[4] · C. A. Cardoso[3] · D. F. M. Neri[5] · M. P. C. Silva[2] · L. B. Carvalho Jr.[2]

Published online: 18 February 2016

Abstract It is reported the synthesis of magnetic nanoparticles via the chemical co-precipitation of Fe^{3+} ions and their preparation by coating them with polyaniline. The electronic micrograph analysis showed that the mean diameter for the nanoparticles is ∼15 nm. FTIR, powder X-ray diffraction and Mössbauer spectroscopy were used to understand the chemical, crystallographic and ^{57}Fe hyperfine structures for the two samples. The nanoparticles, which exhibited magnetic behavior with relatively high spontaneous magnetization at room temperature, were identified as being mainly formed by maghemite (γFe_2O_3). The coated magnetic nanoparticles (sample labeled "mPANI") presented a real ability to bind biological molecules such as trypsin, forming the magnetic enzyme derivative (sample "mPANIG-Trypsin"). The amount of protein and specific activity of the immobilized trypsin were found to be 13 ± 5 μg of protein/mg of mPANI (49.3 % of immobilized protein) and 24.1 ± 0.7 U/mg of immobilized protein, respectively. After 48 days of storage at 4 °C, the activity of the immobilized trypsin was found to be 89 % of its initial activity. This simple, fast and low-cost procedure was revealed to be a promising way

This article is part of the Topical Collection on *Proceedings of the International Conference on the Applications of the Mössbauer Effect (ICAME 2015), Hamburg, Germany, 13-18 September 2015*

✉ J. C. Maciel
jackeline_maciel@hotmail.com

[1] Universidade Federal de Roraima, Campus Paricarana, 69301–000 Boa Vista, Roraima, Brazil

[2] Laboratório de Imunopatologia Keizo Asami, Universidade Federal de Pernambuco, Recife, PE, Brazil

[3] Departamento de Física, Universidade Federal de São Carlos, São Carlos, SP, Brazil

[4] Universidade Federal dos Vales de Jequitinhonha e Mucuri, Diamantina, MG, Brazil

[5] Universidade Federal do Vale do São Francisco, Petrolina, PE, Brazil

to prepare mPANI nanoparticles if technological applications addressed to covalently link biomolecules are envisaged. This route yields chemically stable derivatives, which can be easily recovered from the reaction mixture with a magnetic field and recyclable reused.

Keywords Magnetic nanoparticles · PANI · Trypsin · Biomedical applications

1 Introduction

Magnetic nanomaterials as magnetite, maghemite and metal ferrites has been widely used in biomedicine and in heterogeneous catalysis, due to their unique magnetic properties and multifunctional surface that can be chemically modified [1]. The functionalization of the surface of magnetic iron oxides nanoparticles by organic molecules has been giving rise to intensive searches addressed to biomedical applications such as magnetic drug targeting, hyperthermia and enzyme immobilization [2]. The main interests are due to their unique catalytic, magnetic and electrical behaviors [3]. Within this scope, magnetite (Fe_3O_4) and maghemite (γ-Fe_2O_3) have become the main magnetic iron oxides nanoparticles presenting real potentiality for different technological applications. The main features of magnetite nanoparticles are based on the chemical functionality of their active surface, their biocompatibility, low-cost and the relatively high saturation magnetization [4, 5]. The need for combining the magnetic and electrical conduction properties leads to design and to develop new materials such as magnetic particles anchoring a conductor polymer [6]. Polyaniline (PANI) may be a special focus, among other conductor polymers, taking into account that it may be more easily synthesized, starting from low-cost materials. PANI has good chemical stability and significant ability to be electrically switched between its conductive and resistive states [7]. The electric and magnetic properties of polyaniline can be modified by adding inorganic fillers, as by the inclusion of magnetic particles, intended to improve the magnetic and dielectric properties of host materials [8]. The production of monodisperse nanopowders and the assessment of their composition and sizes distribution are therefore key-points on those applications [9]. The main objective of this work was to produce magnetic nanoparticles coated with PANI to be used as a support for enzyme immobilization, using trypsin as molecule model. For this, magnetic nanoparticles were prepared via the co-precipitation Fe^{2+} and Fe^{3+} ions in aqueous solution. The catalytic performance of the enzyme derivative was then evaluated. These magnetic nanoparticles were also characterized by electronic micrographic observations, FTIR, X-ray diffraction analysis, ^{57}Fe Mössbauer spectroscopy and magnetization measurements.

2 Materials and methods

2.1 Materials

Trypsin (E.C.3.4.21.4) from porcine pancreas, bovine serum albumin (BSA), *N*-benzoyl-D-L-arginine-*p*-nitroanilide (BAPNA), aniline (ACS reagent), potassium permanganate (ACS reagent), Folin-Ciocalteu's phenol reagent and, 25 % glutaraldehyde were purchased from Sigma-Aldrich (USA). Dimethylsulfoxide (DMSO) and sodium hydroxide were from Vetec Chemical (Brazil). Ferric chloride hexahydrate and ferrous chloride tetrahydrate were from Merck (Germany). All other reagents were of analytical grade.

2.2 Magnetic particles preparation

Solutions of 1.1 mol L^1 $FeCl_3$.$6H_2O$ (5 mL) and of 0.6 mol L^{-1} $FeCl_2$.$4H_2O$ (5 mL) were added to 50 mL of distilled water, under magnetic agitation, and 5.0 mol L^{-1} NaOH was added dropwise up to pH 10 when black particles precipitated. The mixture was heated at 50 °C for 30 min with vigorous stirring. The magnetic nanoparticles were thoroughly washed with distilled water until neutral pH. The material was dried up and kept at 25 °C.

2.3 Coating with PANI

Oxidative polymerization of aniline was carried out in the presence of magnetic nanoparticles (0.5 g), then treated with 0.1 mol L^{-1} $KMnO_4$ (50 mL) solution at 25 °C for 1 h and washed with distilled water. Then magnetic-$KMnO_4$ nanoparticles were immersed into 50 mL of 0.5 mol L^{-1} aniline solution (in 1.0 mol L^{-1} HNO_3). Polymerization was allowed to occur at 4 °C for 1 h and after that the magnetic nanoparticles coated with polyaniline (mPANI) were successively washed with distilled water, 0.1 M citric acid and rewashed with distilled water, and finally the material was dried up and kept at 25 °C.

2.4 Trypsin immobilization

mPANI (0.01 g) was incubated with 2.0 % w/v glutaraldehyde (1.0 mL) at 25 °C for 2 h under mild stirring, washed with distilled water and Tris-HCl buffer (0.1 mol L^{-1}, pH 8.0) to remove the glutaraldehyde excess. Then, it was activated with glutaraldehyde (mPANIG), kept in buffer at 4 °C and finally incubated with trypsin (200 μ g/mL) for 16 h at 4 °C under mild stirring. The enzymatic derivative (mPANIG-Trypsin) was collected by a magnetic field (Ciba corning; 0.6 T) and the supernatant and washings were used for protein determination.

2.5 Activity assay

Amidase activity of trypsin was measured by using the artificial substrate BAPNA (4.0 mM in DMSO). The mixture of reaction was incubated at 25 °C for 15 min. The hydrolyzed p-nitroanilide was monitored in spectrophotometer at 440 nm and the activity of enzyme was calculated. All assays were carried out in replicates and the results were expressed as "*mean ±SD*". The activity of trypsin (unit) was defined as μ mol BAPNA hydrolyzed per minute using an absorption coefficient of 9.100 $M^{-1}cm^{-1}$. The specific activity was calculated by dividing the enzymatic activity (U) by the amount of protein (mg). For the residual specific activity the specific activity of free enzyme was considered as 100 %.

2.6 Protein determination

The amount of immobilized protein was estimated by the difference between the offered protein and that found in the supernatant and washing solutions measured according to the method Lowry et al. [10] using bovine serum albumin (BSA) as a standard.

2.7 Magnetic nanoparticles characterization

The morphology and particle size of the nanoparticles were characterized using a Jeol 1200EXII 80 transmission electron microscope (TEM). The Fourier transform infrared

(FTIR) spectra were obtained using an IFS–66 FTIR spectrometer (Bruker, Billerica, MA, USA) in the range of 4000-400 cm^{-1} using KBr pellets. Typically, 100 scans were recorded with a 4 cm^{-1} resolution.

The magnetic particles structural properties were characterized by X-ray powder diffraction, which was carried out in a ray-X diffractometer Shimadzu model XDR 7000, using Cu Kα radiation ($\lambda = 0.154$ nm) at a scanning speed of 0.1° s^{-1} in the range of $2\theta = 10$–90° with a 0.02° step.

Mössbauer spectra were recorded with a constant acceleration transmission mode setup, at room temperature, using a 10 mCi ^{57}Co (Rh-matrix) source. The Doppler velocity scale of the Mössbauer spectrometer (model MB500) was calibrated by using a thin α-Fe foil as absorber. Data analysis was performed using the computer program WinNormos for IGOR Pro 6.36 assuming Lorentzian functions, through the least-square convergence fitting.

Magnetization measurements were obtained at 298 K and 323 K in ˜5 T applied field using a SQUID magnetometer (Quantum Design Model MPMS-5S).

2.8 Chemical stability during storage and reuse

The mPANIG-Trypsin was stored in Tris-HCl buffer at 4 °C. The remaining activity of immobilized trypsin (item 2.5) was evaluated for 6 subsequent cycles during 55 days measuring its activity followed by Tris-HCl buffer washing and storage again in the buffer at 4 °C.

3 Results and discussion

3.1 Synthesis of magnetic nanoparticles and PANI coating

According to Sun et al. [11], the synthesis of magnetic particles with sizes around 10 nm was achieved using a reaction temperature of 50 °C, a solution at pH 10–11 and a high stirring rate (above 800 rpm). According to those authors, temperatures above 50 °C produce larger particles. At pH values between 10 and 11, smaller magnetic nanoparticles are obtained. This can be explained by means of the chemical mechanism to form the magnetic particles [12]. In order to obtain nanoparticles, the synthesis protocol of magnetic particles [11], which is generally used in our laboratory was modified so to use the incubation time of 30 min, at 50 °C, with the final pH of the mixture reaching 10, and NaOH as the co-precipitation agent.

NaOH was chosen as the precipitating agent instead of $NH_4{\cdot}OH$ as used by Carneiro Leão et al. [11], as according to Hong et al. [13] the magnetite nanoparticles shows minor agglomeration and smaller diameter if NaOH is used. The magnetic nanoparticles produced in this work (mean diameter, ˜15 nm) have dimensions much smaller than those obtained by Neri et al. [14] (10–100 µm) who followed the protocol reported by Carneiro Leão et al. [11]. Roth et al. [15] performed the synthesis of superparamagnetic nanoparticles by the co-precipitation of Fe^{2+} and Fe^{3+} in aqueous alkaline environment (NaOH) and obtained nanoparticles between 3 and 17 nm, a particle size range comparable to that found in this study (Fig. 1).

The magnetic nanoparticles produced were coated with PANI (mPANI) by the oxidation of aniline with potassium permanganate, producing PANI in form of emeraldine, that is the most stable and conductive [7]. It is well known that, under certain synthesis conditions, PANI forms a sub-micrometer film on the surface of the objects immersed into the

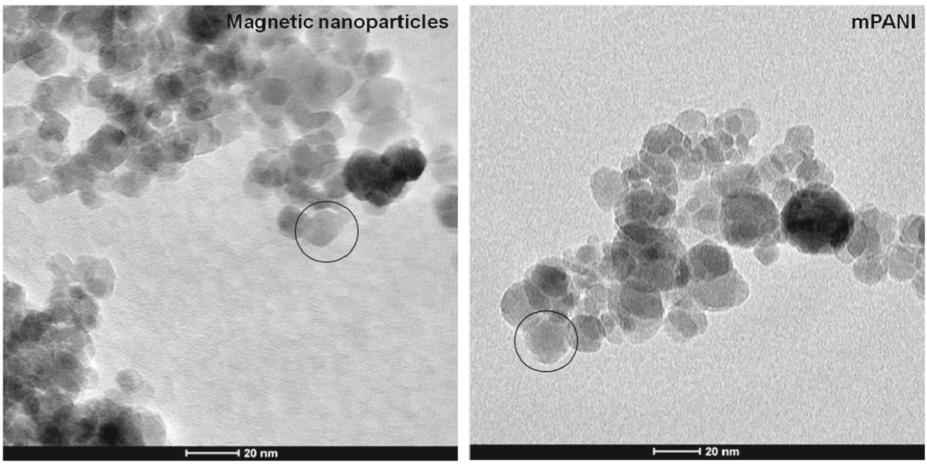

Fig. 1 Electron microscopic images. TEM image of magnetic nanoparticles and mPANI. The *circle* on the figures indicate isolated magnetic nanoparticle

polymerization mixture. These films are formed on various types of substrates: conducting, insulating, hydrophobic, and hydrophilic. The parameters of the film (thickness, uniformity, and morphology) depend both on the chemical nature of the coated surface and on the synthesis conditions [16]. While hydrophobic materials are covered by a more or less uniform PANI film, the film relief on hydrophilic microparticles has often a discontinuous patchy character [17]. In this work it was observed that besides the covering process a PANI precipitate was produced. This residue was easily removed from the magnetic nanoparticles surface by washing under a magnetic field. The ratio between the amounts of precipitate and film depends on the synthesis conditions [18]. Previous mechanism [14] was used to produce particles composed of a magnetic core (iron oxide) and an organic shell (PANI). Here, the optimal conditions of the coating process were established by using an experimental design (results not shown). These conditions were: 0.1 M $KMnO_4$, 0.5 M aniline, contact time of $KMnO_4$ of 1 h, polymerization time of 1 h and polymerization temperature at 4 °C. The concentrations of the oxidizing agent and aniline were identical to the protocol; however, the contact time of $KMnO_4$ was reduced from overnight to 1 h, the polymerization time from 2 to 1 h and, the polymerization temperature from 25 to 4 °C. The morphology, shape and size distribution of magnetic nanoparticles and mPANI were examined by transmission electron microscopy (TEM) and typical images are shown in Fig. 1. The magnetic nanoparticles exhibited agglomerates with apparently regular morphology, nearly spherical/ellipsoidal shape, dimensions around 15 nm, and narrow particle size distribution (Fig. 1).

3.2 FTIR spectra

The emeraldine salt is the partly oxidized form of polyaniline where six benzene rings and two quinoid rings are present in an eight-ring repeating unit. The conductivity of the emeraldine form of polyaniline can be changed by about 10 orders of magnitude by doping [19]. The FTIR spectra of magnetic nanoparticles and mPANI are shown in Fig. 2. It was found that mPANI had characteristic peaks at around 1494 cm^{-1} (C = C stretching of benzenoid ring), 1398 cm^{-1} (Q = N–B stretching deformation, Q refers to the quinoid ring

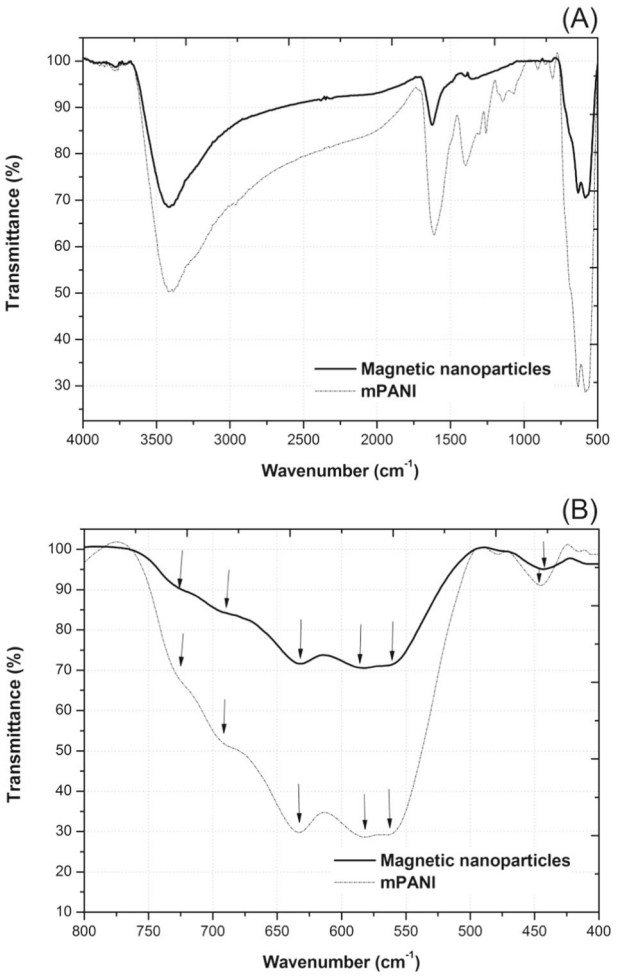

Fig. 2 FTIR spectra (**a**) and absorption bands of 750 – 400 cm^{-1} (**b**) of magnetic nanoparticles and mPANI

and B to the benzenoid ring), 1305 and 1260 cm^{-1} (C–N stretching benzenoid ring) and 805 cm^{-1} (out-of-plane deformation of C–H in the 1, 4-disubstitued benzene ring), which was similar with polyaniline [14, 20, 21].

Polymerization proceeds initially on the surface of these oxide particles in the presence of $KMnO_4$. The adsorption of polymer to the magnetic nanoparticles results in constrained chain growth around the particles. Such adsorption and constrained motion of the chains will restrict the modes of vibration in polyaniline, which in turn lead to the reduction in intensity in the FTIR spectra [19, 22]. The presence of Fe–O bond in particles can be seen by two strong absorption bands at around 635 and 590 cm^{-1}. These bands result from split of the ν_1 band at 570 cm^{-1}, which corresponds to the Fe–O bond of bulk magnetite [23–26]. The absorption bands of Fe–O bond were observed around 631 and 588 cm^{-1} for magnetic nanoparticles and 630 and 580 cm^{-1} for mPANI. A principal effect of finite size of nanoparticles is the breaking of large number of bonds for surface atoms, resulting in the

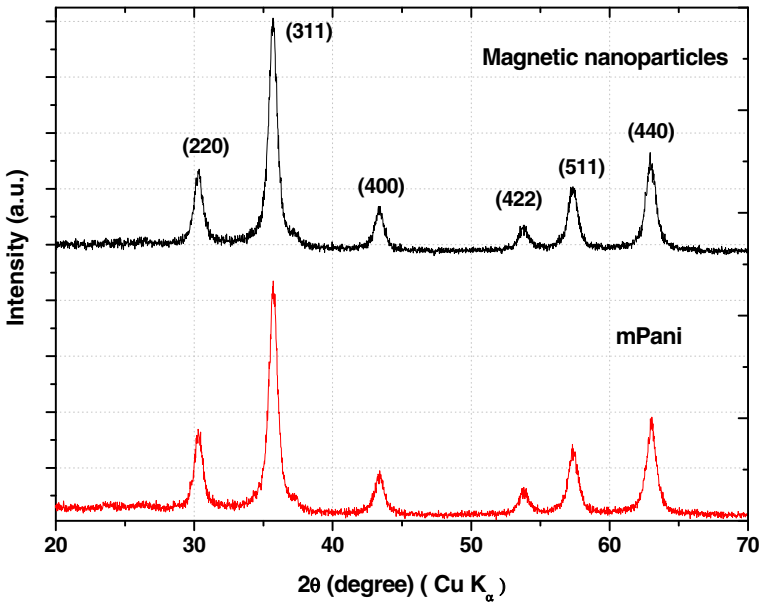

Fig. 3 XRD patterns of magnetic nanoparticles and mPANI

rearrangement of electrons on the particle surface [23]. The FTIR spectra in the range 750–450 cm^{-1} for magnetic nanoparticles and mPANI are shown in the Fig. 2b. These spectra are compared with the spectrum of maghemite (not shown) confirming the oxidation and its increase after coating (Fig. 2b). The spectra exhibit absorption bands around the 570 cm^{-1} characteristic of magnetite [9]. Moreover, the bandwidth increases, and small shoulders in the 600–750 cm^{-1} range as well as a band at 450 cm^{-1} appear with greater intensity after coating of the magnetic particles. The appearance of the characteristic maghemite peaks seems to promote coating. So, FTIR spectra indicate the presence of magnetite and/or maghemite in the samples.

3.3 XRD analysis

Colors of iron oxide may be very dependent on grain size and chemical composition and this feature is a first auxiliary attribute in their identification [27]. The magnetic nanoparticles and mPANI were very dark and magnetic, suggesting that magnetite could be the dominant phase, although maghemite may not be excluded. Figure 3 shows XRD patterns for magnetic nanoparticles and mPANI. The 2θ peaks at 18.44, 30.30, 35.67, 43.37, 53.80, 57.35, 62.97, 71.43 and 74.48° [3, 28–31] are attributed to the crystal planes at (111), (220), (311), (400), (422), (511), (440), (620) and (533) [32], which can refers to both, magnetite and maghemite, according to the International Center for Diffraction Data (reference code: ICDD 019-0629). As observed by Andrade et al. [27] no clear reflection peak due to other crystalline phase, which could occur as impurity, was observed, indicating that final products were pure enough, from this point of view, consisting essentially of binary mixture of the two spinel magnetic iron oxides, meaning magnetite and maghemite. In this way, XRD results confirm FTIR results. Furthermore, the results show broadened lines that can be

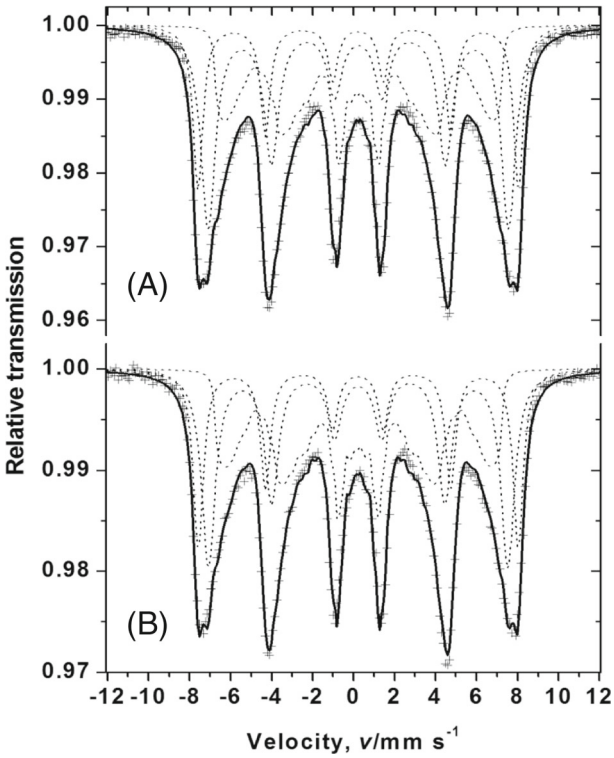

Fig. 4 298 K-Mössbauer spectra for the (**a**) magnetic nanoparticles and (**b**) mPANI samples

due to the magnetization relaxation from superparamagnetism and matrix constritions for nanosized particles [33].

3.4 Mössbauer spectroscopy (MS)

Magnetite ($[Fe^{3+}]\{Fe^{2+}Fe^{3+}\}O_4$, where [ ] and { } stand for tetrahedral and octahedral symmetries of the coordination polyhedral Fe-O) and maghemite (ideal formula, $[Fe^{3+}]\left\{Fe^{3+}_{\frac{5}{3}}\oplus_{\frac{1}{3}}\right\}O_4$, where $\oplus$ = cation vacancy; stoichiometrically, it corresponds to the γFe_2O_3) have cubic unit cells with close dimensions. These circumstances render very similar XRD patterns. On the other hand, maghemite contains only Fe^{3+} whereas magnetite has Fe^{3+} and Fe^{2+} in the spinel structure. Mössbauer spectroscopy can thus give a direct assessment of the chemical state of iron, which may distinguish between the two iron oxides nanoparticles. The used fitting model for these Mössbauer patterns (Fig. 4), with relatively asymmetric resonance lines, was mainly based on two sextets (subspectral areas of 81.4 and 82.9 % for the sample containing the sole magnetic nanoparticles and for the magnetic nanoparticles coated with with polyaniline—the mPANI sample, respectively) with Lorentzian lines (fitted spectra are shown in Fig. 4; corresponding Mössbauer parameters are presented in Table 1). The remaining area of the two spectra (18.6 and 17.1 % for the sole magnetic and for the polyaniline coated magnetic nanoparticles, respectively) were completed by fitting them with model-independent hyperfine field distributions. Figures

Table 1 Fitted hyperfineparameters for the 298 K-Mössbauer spectra

Sample	^{57}Fe site	δ /mm s $^{-1}$	$2\varepsilon_Q$ /mm s $^{-1}$	Γ/mm s $^{-1}$	B_{hf}/T	RA/%
Magnetic nanoparticles	[Fe^{3+}]	0.329(2)	−0.010(5)	0.86(2)	45.45(5)	47.0
	{Fe^{3+}}	0.319(2)	−0.001(1)	0.57(1)	48.49(3)	34.4
mPANI	[Fe^{3+}]	0.321(2)	−0.0075(5)	0.85(2)	45.28(5)	45.6
	{Fe^{3+}}	0.319(2)	−0.001(1)	0.60(1)	48 × (3)	37.3

δ = isomer shift relative to αFe; $2\varepsilon_Q$ = quadrupole shift; Γ = resonance linewidth; B_{hf} = hyperfine field; RA = relative subspectral area. [ ] and { } denotes tetrahedral and octahedral symmetries, respectively, for the Fe-O coordination sites. Numbers in parentheses are uncertainties over the last significant digit of the numerical value, as output by the least squares fitting computer program

of the corresponding hyperfine field probability profiles are not shown. The found isomer shift values are characteristic of high spin Fe^{3+}. The fitted values of quadrupole shift are consistent with those expected for iron spinels. The hyperfine field relative to the two sextets for each sample correspond to the tetrahedral and octahedral Fe^{3+} sites in nanosized maghemite. The decrease in the fitted hyperfine field B_{hf} for both sites (45.3 and 48.4 T) relatively to pure oxide (nearly 50 T) is consistent with the expected effect due to the collective magnetic excitations [34]. From these Mössbauer data, the occurrence of magnetite can be safely discarded in these two samples. Moreover, Mössbauer results indicate that coating with mPANI does not significantly alter the chemical nature of the produced oxide [35].

3.5 Magnetization measurements

The magnetic properties of the magnetic nanoparticles and mPANI were investigated in the applied magnetic field sweeping from −60 to 60 kOe at 298 K and 323 K as shown in Fig. 5. It is well-known that the size [36], structure and shape may affect the magnetic properties of the products [37]. Under applied magnetic field, magnetic nanoparticles and mPANI showed the positive magnetizations and there is no hysteresis (Fig. 5). It indicates the superparamagnetic behavior [25]. The difference between the magnetic behavior of small and medium sized particles can also be observed in their hysteresis loops [9].

Figure 5 shows the field dependent magnetization curves of magnetic nanoparticles and mPANI. The saturation magnetization (M_s) for the magnetic nanoparticles has value equal to 60.51 emu g^{-1}, which is lower than that of bulk magnetite (M_s = 92 emu g^{-1}) [38], and mPANI has value equal to 59.05 emu g^{-1} (Fig. 5). The reduction in the saturation magnetization values signifies the decrease in the particles size [39] and can be attributed to surface effects such as magnetically inactive layer containing spins that are not collinear with the magnetic field. These discrepancies in the saturation values of magnetization may be explained by variations in the methods employed to synthesize magnetite, which can generate different particle sizes, magnetite surfaces and chemical compositions [40].

3.6 Stability during storage and reuse

Data of operational stability showed that after 5 cycles combining storage and reuse, mPANIG-Trypsin maintained 89 % of its initial activity (Fig. 6). An 11 % decrease in activity was detected during this period. The immobilized trypsin on polyaniline supports retained 50 % its original activity after 21 days when stored at 4 °C in phosphate buffer

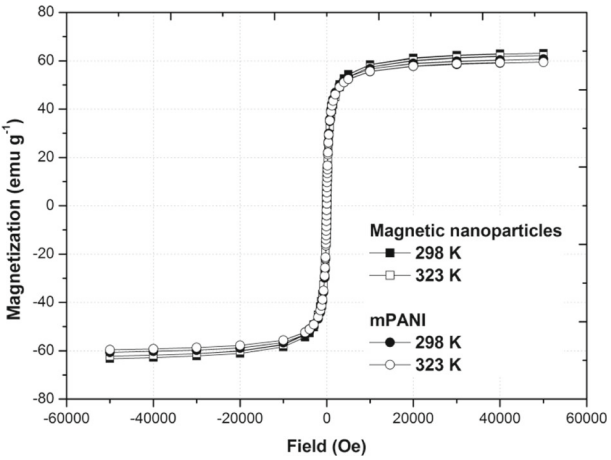

Fig. 5 Magnetization curves of magnetic nanoparticles and mPANI at 298 and 323 K

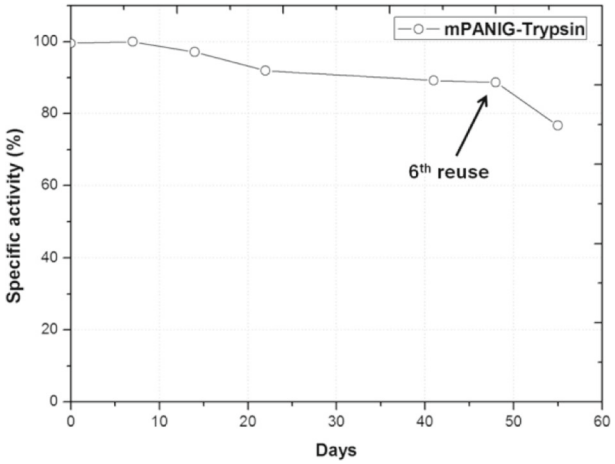

Fig. 6 Shelf life of mPANIG-Trypsin at 4 °C stored in Tris-HCl buffer

[41], 58 % its original activity after 49 days when stored at 4 °C in glycine buffer containing $CaCl_2$ [42] and 80 % its original activity after 44 days (approximately) when stored in glycine buffer containing $CaCl_2$ [43]. Sun et al. [44] conducted the immobilization of trypsin onto the superparamagnetic carboxymethyl chitosan and the immobilized enzyme exhibited stability for six times reuse, holding 76.3 % of its initial activity. In our study, we observed better results. Moreover, Chellapandian [45] reported that immobilized trypsin on vermiculite retained 84 % its original activity after 60 days when stored in borate buffer. The enzymatic derivative obtained this study was more stable during the period of 48 days, however its activity after 55 days was 77 % of initial value. This result indicates that the mPANIG-Trypsin may be stored in buffer only (no stabilizer, e.g. $CaCl_2$) for approximately 50 days, retaining about 90 % of its initial activity.

4 Conclusions

In conclusion, magnetic nanoparticles were obtained from modifications of the experimental protocol used routinely by our research group. These nanoparticles showed dimensions smaller than those obtained by original the protocol, corroborating the advantages of the optimization process. The FTIR, XRD and Mössbauer spectroscopy analysis of the nanoparticles confirmed the presence of maghemite. Furthermore, after PANI coating, nanoparticles preserved good magnetization, an increase in the surface area and showed to be an excellent support for trypsin immobilization. The major benefits of the magnetic enzymatic derivative (mPANIG-Trypsin) are its operational stability, high activity, simple method and low cost of production.

Acknowledgments The authors wish to acknowledge financial support from the Brazilian agency CNPq (Conselho Nacional de Desenvolvimento Científico e Tecnológico) and FACEPE (Fundação de Amparo a Ciência e Tecnologia de Pernambuco). The authors would like to thank Prof. Dr. Márcia Attias (Laboratório de Ultraestrutura Celular Herta Meyer, UFRJ, Brazil) for the transmission electron microscopy analysis, Prof. Dr. Adilson J.A. de Oliveira (UFSCar, SP, Brazil) for the magnetization measurements. CAPES (Brazil) grants the Visiting Professor PVNS fellowship to JDF at UFVJM.

References

1. Reddy, L.H., Arias, J.L., Nicolas, J., Couvreur, P.: Magnetic nanoparticles: design and characterization, toxicity and biocompatibility, pharmaceutical and biomedical applications. Chem. Rev. **112**, 5818–5878 (2012)
2. Daou, T.J., Grenèche, J.M., Pourroy, G., Buathong, B., Derory, A., Ulhaq-Bouillet, C., Donnio, B., Guillon, D., Begin-Colin, S.: Coupling agent effect on magnetic properties of functionalized magnetite-based nanoparticles. Chem. Mater. **20**, 5869–5875 (2008)
3. Gu, H., Huang, Y., Zhang, X., Wang, Q., Zhu, J., Shao, L., Haldolaarachchige, N., Young, D.P., Wei, S., Guo, Z.: Magnetoresistive polyaniline-magnetite nanocomposites with negative dielectrical properties. Polymer **53**, 801–809 (2012)
4. Salado, J., Insausti, M., Lezama, L., de Muro, I.G., Goikolea, E., Rojo, T.: Preparation and characterization of monodisperse Fe_3O_4 nanoparticles: na electron magnetic resonance study. Chem. Mater. **23**, 2879–2885 (2011)
5. Belaabed, B., Wojkiewicz, J.L., Lamouri, S., Kamchi, N.E., Lasri, T.: Synthesis and characterization of hybrid conducting composites based on polyaniline/magnetite fillers with improved microwave absorption properties. J. Alloy Compd. **527**, 137–144 (2012)
6. Khafagy, R.M.: Synthesis, characterization, magnetic and electrical properties of the novel conductive and magnetic Polyaniline/$MgFe_2O_4$. J. Alloy Compd. **509**, 9849–9857 (2011)
7. Balint, R., Cassidy, N.J., Cartmell, S.H.: Conductive polymers: towards a smart biomaterial for tissue engineering. Acta Biomater. **10**, 2341–2353 (2014)
8. Gandhi, N., Singh, K., Ohlan, A., Singh, D.P., Dhawan, S.K.: Thermal, dielectric and microwave absorption properties of polyaniline–$CoFe_2O_4$ nanocomposites. Compos. Sci. Technol. **71**, 1754–1760 (2011)
9. Salazar, J.S., Perez, L., Abril, O., Phuoc, L.T., Ihiawakrim, D., Vazquez, M., Greneche, J.-M., Begin-Colin, S., Pourroy, G.: Magnetic iron oxide nanoparticles in 10–40 nm range: composition in terms of magnetite/maghemite ratio and effect on the magnetic properties. Chem. Mater. **23**, 1379–1386 (2011)
10. Lowry, O.H., Rosebrough, N.J., Farr, A.L., Randall, R.J.: Protein measurement with the Folin phenol reagent. J. Biol. Chem. **193**, 265–275 (1951)
11. Carneiro Leão, A.M.A., Oliveira, E.A., Carvalho Jr., L.B.: Immobilization for protein on ferromagnetic Dacron. Appl. Biochem. Biotech. **32**, 53–58 (1991)
12. Sun, J., Zhou, S., Hou, P., Yang, Y., Weng, J., Li, X., Li, M.: Synthesis and characterization of biocompatible Fe_3O4 nanoparticles. J. Biomed. Mater. Res. A **80A**, 333–341 (2007)
13. Hong, R., Li, J., Wang, J., Li, H.: Comparison of schemes for preparing magnetic Fe_3O4 nanoparticles. China Part **5**, 186–191 (2007)

14. Neri, D.F.M., Balcão, V.M., Dourado, F.O.Q., Oliveira, J.M.B., Carvalho Jr., L.B., Teixeira, J.A.: Immobilized β-galactosidase onto magnetic particles coated with polyaniline: support characterization and galactooligosaccharide production. J. Mol. Catal. B-Enzym. **70**, 74–80 (2011)
15. Roth, H.-C., Schwaminger, S.P., Schindler, M., Wagner, F.E., Berensmeier, S.: Influencing factors in the co-precipitation process of superparamagnetic iron oxide nanoparticles: a model based study. J. Magn. Magn. Mater. **377**, 81–89 (2015)
16. Stejskal, J., Sapurina, I., Prokeš, J., Zemek, J.: In-situ polymerization polyaniline films. Synthetic Met. **105**, 195–202 (1999)
17. Kohut-Svelko, N., Reynaud, S., Dedryevre, R., Martinez, H., Gonbeau, D., Francois, J.: Study of a nanocomposite based on a conducting polymer: polyaniline. Langmuir **21**, 1575–1583 (2005)
18. Stejskal, J., Trchová, M., Fedorova, S., Sapurina, I., Zemek, J.: Surface polymerization of aniline on silica gel. Langmuir **19**, 3013–3018 (2003)
19. Nagaraja, N., Pattar, J., Shashank, N., Manjanna, J., Kamada, Y., Rajanna, K., Mahesh, H.M.: Electrical, structural and magnetic properties of polyaniline/pTSA-TiO_2 nanocomposites. Synthetic Met. **159**, 718–722 (2009)
20. Xiao, Q., Tan, X., Ji, L., Xue, J.: Preparation and characterization of polyaniline/nano-Fe_3O4 composites via a novel Pickering emulsion route. Synthetic Met. **157**, 784–791 (2007)
21. Lin, Y.-W., Wu, T.-M.: Synthesis characterization of externally doped sulfonated polyaniline/multi-walled carbon nanotube composites. Compos. Sci. Technol. **69**, 2559–2565 (2009)
22. Feng, W., Bai, X.D., Lian, Y.Q., Liang, J., Wang, X.G., Yoshino, K.: Well-aligned polyaniline/carbon-nanotube composite films grown by in-situ aniline polymerization. Carbon **41**, 1551–1557 (2003)
23. Ma, M., Zhang, Y., Yu, W., Shen, H., Zhang, H., Gu, N.: Preparation and characterization of magnetite nanoparticles coated by amino silane. Colloid Surface A **212**, 219–226 (2003)
24. Xu, X.Q., Shen, H., Xu, J.R., Li, X.J.: Aqueous-based magnetite magnetic fluids stabilized by surface small micelles of oleolysarcosine. Appl. Surf. Sci. **221**, 430–436 (2004)
25. Yamaura, M., Camilo, R.L., Sampaio, L.C., Macêdo, M.A., Nakamura, M., Toma, H.E.: Preparation and characterization of (3-aminopropyl) triethoxysilane-coated magnetite nanoparticles. J. Magn. Magn. Mater. **279**, 210–217 (2004)
26. Klokkenburg, M., Hilhorst, J., Erné, B.H.: Surface analysis of magnetite nanoparticles in cyclohexane solutions of oleic acid and oleylamine. Vib. Spectrosc. **43**, 243–248 (2007)
27. Andrade, A.L., Valente, M.A., Ferreira, J.M.F., Fabris, J.D.: Preparation of size-controlled nanoparticles of magnetite. J. Magn. Magn. Mater. **324**, 1753–1757 (2012)
28. Reddy, K.R., Lee, K.-P., Gopalan, A.I., Kang, H.-D.: Organosilane modified magnetite nanoparticles/poly(aniline-co-o/m-aminobenzenesulfonic acid) composites: synthesis and characterization. React. Funct. Polym. **67**, 943–954 (2007)
29. Yu, W., Zhang, T., Zhang, J., Qiao, X., Yang, L., Liu, Y.: The synthesis of octahedral nanoparticles of magnetite. Mater. Lett. **60**, 2998–3001 (2006)
30. Xu, F., Ma, L., Hu, Q., Gan, M., Tang, J.: Microwave absorbing properties and structural design of microwave absorbers based on polyaniline and polyaniline/magnetite nanocomposite. J. Magn. Magn. Mater. **374**, 311–316 (2015)
31. Vandenberghe, R.E., Barrero, C.A., da Costa, G.M., Van San, E., De Grave, E.: Mössbauer characterization of iron oxides and (oxy)hydroxides: the present state of the art. Hyperfine Interact **126**, 247–259 (2000)
32. Klug, H.P., Alexander, L.E. X-ray Diffraction Procedures for Polycrystalline and Amorphous Materials, 2nd edn. Willey-Interscience, New York (1974)
33. Quin, X.Y.: The exothermal and endothermal phenomena in nanocrystalline aluminum. Nanostruct. Mater. **2**, 99–106 (1993)
34. Mørup, S., Frandsen, C., Hansen, M.F.: Magnetic interactions between nanoparticles. Beilstein J. Nanotechnol. **1**, 48–54 (2010)
35. Jaramillo-Tabares, B.E., Isaza, F.J., Córdoba de Torresi, S.I.: Stabilization of polyaniline by the incorporation of magnetite nanoparticles. Mater. Chem. Phys. **132**, 529–533 (2012)
36. Wen, X., Yang, J., He, B., Gu, Z.: Preparation of monodisperse magnetite nanoparticles under mild conditions. Curr. Appl. Phys. **8**, 535–541 (2008)
37. Xu, H., Shao, M., Chen, T., Zhuo, S., Wen, C., Peng, M.: Magnetism-assisted assembled porous Fe_3O4 nanoparticles and their electrochemistry for dopamine sensing. Micropor. Mesopor. Mat. **153**, 35–40 (2012)
38. Cullity, D.: Introduction to Magnetic Materials. Addison-Wesley, Reading, MA (1972)
39. Xu, L., Du, J., Li, P., Qian, Y.: In situ synthesis, magnetic property, and formation mechanism of Fe_3O4 particles encapsulated in ID bamboo-shaped carbon microtubes. J. Phys. Chem. B **110**, 3871–3875 (2006)

40. Grigorova, M., Blythe, H.J., Blaskov, V., Rusanov, V., Petkov, V., Masheva, V., Nihtianova, D., Martinez, L.M., Muñoz, J.S., Mikhov, M.: Magnetic properties and Mössbauer spectra of nanosized $CoFe_3O4$ powders. J. Magn. Magn. Mater. **183**, 163–172 (1998)
41. Caramori, S.S., Fernandes, K.F.: The use of poly(ethylene terephthalate)-poly(aniline) composite for trypsin immobilization. Mater. Sci. Eng. C **28**, 1159–1163 (2008)
42. Purcena, L.L.A., Caramori, S.S., Mitidieri, S., Fernandes, K.F.: The immobilization of trypsin onto polyaniline for protein digestion. Mater. Sci. Eng. C **29**, 1077–1081 (2009)
43. Caramori, S.S., Faria, F.N., Viana, M.P., Fernandes, F.K., Carvalho, J.r., L.B.: Trypsin immobilization on discs of polyvinyl alcohol glutaraldehyde/polyaniline composite. Mater. Sci. Eng. C **31**, 252–257 (2011)
44. Sun, J., Hu, K., Liu, Y., Pan, Y.: Novel superparamagnetic nanoparticles for trypsin immobilization and the application for efficient proteolysis. J. Chromatography B **942–943**, 9–14 (2013)
45. Chellapandian, M.: Preparation and characterization of alkaline protease immobilized on vermiculate. Process Biochem. **33**, 169–173 (1998)